Research Article Adv. Mat. Lett. 2012, **3**(5), 399-405 ADVANCED MATERIALS Letters

www.amlett.org, www.amlett.com, DOI: 10.5185/amlett.2012.7288 Published online by the VBRI press in 2012

Induced size effects of Gd^{3+} ions doping on structural and magnetic properties of Ni-Zn ferrite nanoparticles

Balwinder Kaur[1], Manju Arora[2], Ajay Shankar[2], Avanish Kumar Srivastava[2,*] and Rajendra Prasad Pant[2]

[1]*G.G.M. Science College, Canal Road, Jammu (J&K) 180001, India*

[2]*National Physical Laboratory, Council of Scientific and Industrial Research, Dr. K.S. Krishnan Road, New Delhi 110012, India*

[*]Corresponding author. Tel: (+91) 11-45609308; Fax: (+91) 11-45609310; E-mail: aks@nplindia.ernet.in

ABSTRACT

Gd^{3+} ions substituted in $Ni_{0.5}Zn_{0.5}Gd_xFe_{2-x}O_4$ (where x = 0.1, 0.2, 0.3) ferrite nanoparticles in the size range from 15 to 25 nm were prepared by chemical method. The effect of Gd^{3+} ions in spinel structure in correlation to structural and magnetic properties have been studied in detail using XRD, HRTEM and EPR techniques. The spin resonance confirms the ferromagnetic behaviour of these nanoparticles and higher order of dipolar-dipolar interaction. On increasing Gd^{3+} ions concentrations, the super exchange interaction i.e. increase in movement of electron among Gd^{3+} - O - Fe^{3+} in the core group and the spin biasing in the glass layer has been interpreted. The decrease in 'g' value and increase in relaxation time is well correlated with the change of particle size on different concentrations of Gd^{3+} ions in Ni-Zn ferrite.

Keywords: Spinel ferrite; nanoparticles; HRTEM, EPR; g – value; resonance field; line width.

A. K. Srivastava did Ph.D. at IISc Bangalore, (Metallurgy), M.Tech. at IIT, Kanpur (Materials Science), M.Sc. at IIT, Roorkee (Physics). He has collaborations with IISc Bangalore, BHU Varanasi, IIT Delhi, IIT Kanpur, University of Paris (France), University of Reims (France), Technical University Darmstadt (Germany), University of Arkansas (USA), University of Okayama (Japan) and POSTECH (South Korea). He has about 110 publications in highly reputed international journals like NanoLetters, Nanotechnology, Acta Materialia, Small, etc. and proceedings. He is DST (Govt. of India) BOYSCAST fellow. He is the recipient of INSA-fellowship under International bilateral exchange program. He has been awarded the Materials Research Society of India – Medal - 2011 and Metallurgist of the Year – 2011, Ministry of Steel, Government of India.

R. P. Pant, Head EPR Spectroscopy and Magnetic fluid Group National Physical laboratory,New Delhi- is carrying out work on the synthesis and characterization of nanomagnetic particles,ferrofluids and their device. The research is focused on the structural and magnetic characterization of particles. The lab is equipped with Bruker make X& Q band along with ENDOR facility and UV irradiation set up in the temp range 4K-350 K .The Anton par Magnetorheometer with all rheological attachment is used to study the flow properties.

Ajay Shankar, CSIR-SRF, National Physical Laboratory, New Delhi, is working in the area Nanomagnetic particles, ferrofluids. The investigations on size induced effect on particles size by electron paramagnetic resonance techniques is the main area of research. Also the rheological study of particles is of area of research interest.

Introduction

Ni-Zn ferrites are materials having many technical applications, especially in high frequency fields, due to their reduced magnetic losses [**1**]. The magnetic properties of the nanosized ferrites are entirely different from those of their bulk counterparts, such as the superparamagnetic behavior and associated properties. Nanosized ferrites with uniform particle size and narrow size distribution are desirable for a variety of applications like targeted drug delivery, ferrofluids, medical imaging and other biomedical applications, magnetic data storage, etc. [**2-6**]. Ni – Zn ferrite is a mixed spinel in which the tetrahedral (A) sites are occupied by Zn^{2+} and Fe^{3+} ions and the octahedral (B) sites are occupied by Ni^{2+} and Fe^{3+} ions in the spinel formula of AB_2O_4. A general structural diagram of a spinel structure has been shown in **Fig. 1** [**7**]. $NiZnFe_2O_4$ belongs to spinel structure with formula, $[Fe^{3+}_{1-x}Zn^{2+}_x]^{tet}[Ni^{2+}_{1-x}Fe^{3+}_{1+x}]^{oct}O_4$. $[Fe^{3+}_{1-x}Zn^{2+}_x]$ where $[Fe^{3+}_{1-x}Zn^{2+}_x]$ ions occupy the tetrahedral sites and $[Ni^{2+}_{1-x}Fe^{3+}_{1+x}]$ ions occupy

the octahedral sites [**8,9**]. The distribution of the cations in the tetrahedral and octahedral sites mainly depends on the synthesis process especially when the particles are in the nanometer scale [**8**]. They are being used in the electronic and engineering industry for its good magnetic and dielectric properties. There are various techniques to synthesize nanoferrites such as co-precipitation, thermal decomposition, sol–gel and hydrothermal methods. Among these, chemical technique is suitable to control the particles and their size distribution.

Previous reports [**10-13**] indicate that the integration of rare earth cations into the spinel structure of Ni-Zn ferrite results in modification of basic electrical and magnetic properties. They showed a lowering of the curie temperature and saturation magnetization due to the substitution of iron with lanthanides, the formation of a plateau in the temperature dependent initial permeability curve and an increase in the specific dc resistivity. Additionally microstructural parameters like grain size and porosity were affected.

In the present work, different concentrations of Gd^{3+} are substituted at the lattice of Ni-Zn ferrite to understand the effect of Gd^{3+} content on structural and magnetic properties. The Gd^{3+} substituted Ni-Zn ferrite with composition $Ni_{0.5}Zn_{0.5}Gd_xFe_{2-x}O_4$ (where x = 0.1, 0.2, 0.3) were synthesized by chemical co-precipitation technique. By using this technique, particle size, chemical homogeneity and degree of agglomeration can be easily controlled. The prepared samples were investigated employing XRD, HRTEM and EPR spectroscopy to elucidate the influence of Gd^{3+} ions on the structural and magnetic properties of Ni-Zn ferrite system.

Experimental

Materials synthesis

Nanocrystalline samples of gadolinium substituted NiZn ferrite with composition $Ni_{0.5}Zn_{0.5}Gd_xFe_{2-x}O_4$ (where x = 0.1, 0.2, 0.3) were synthesized by co – precipitation technique. The starting material used were AR grade $Ni(NO_3)_2.6H_2O$, $Zn(NO_3)_2.6H_2O$, $Gd(NO_3)_3.5H_2O$ and $Fe(NO_3)_3.9H_2O$. One molar aqueous solutions were prepared and mixed in respective stoichiometry and homogenized at 60 ^{0}C. The $Ni_{0.5}Zn_{0.5}Gd_xFe_{2-x}O_4$ was precipitated by adding 25% ammonia solution drop wise with constant stirring. The pH of the solution was maintained at 9. The precipitated particles were then washed several times with hot double distilled water to remove the salt residues and other impurities. The precipitated particles were then dried at 80 ^{0}C to obtain the powder. Formation of ferrite nanoparticles is two steps process: first, conversion of metal salts into hydroxides (co-precipitation step) and second, transformation of hydroxides into nanoferrites (fertilization step). The hydroxides of metals in the form of fine particles were obtained by the co–precipitation of metal cations in alkaline medium. This is a fast process. The solid solution of metal hydroxides was then transferred to Ni-Zn ferrite when heated in the alkaline medium at 80 ^{0}C. It requires sufficient time to convert metal hydroxides into ferrites. The overall chemical reactions can be summarized as:

$$Ni^{2+} + (1\text{-}x)Zn^{2+} + yGd^{3+} + (2\text{-}y)Fe^{3+} + 8OH^- \rightarrow xNi(OH)_2(1\text{-}x)Zn(OH)_2yGd(OH)_3(2\text{-}y)Fe(OH)_3$$

$$xNi(OH)_2(1\text{-}x)Zn(OH)_2yGd(OH)_3(2\text{-}y)Fe(OH)_3 \xrightarrow{heat} Ni_xZn_{1-x}Gd_yFe_{2-y}O_4 + 4H_2O$$

These samples were annealed at different temperatures to improve the crystallinity of the material.

Materials characterization

The crystalline phase and make structural parameters are analyzed by using a Rigaku powder X – ray diffractometer at 40 kV and 30 mA, using Cu k_α (λ=1.54059 Å) radiation as an X – ray source in the 2θ range from 20^0 to 70^0 with maintaining step size rate 0.02 ^{0}/S. The shape, size distribution of $Ni_{0.5}Zn_{0.5}Gd_xFe_{2-x}O_4$ (where x = 0.1, 0.2, 0.3) ferrite nanoparticles was carried out with the help of high resolution transmission electron microscope (HRTEM) model: Tecnai G2 F30 STWIN, electron accelerating voltage of 300 kV with FEG source). EPR spectrum of samples of different Gd^{3+} substituted Ni-Zn nanoferrite particles was recorded on X- and Q- band EPR Spectrometer Model: A300 Make: Bruker Biospin, Germany at ambient temperature to study the behavior of magnetic dipolar and superexchange interactions. DPPH was used as a standard reference material for the determination of g-value.

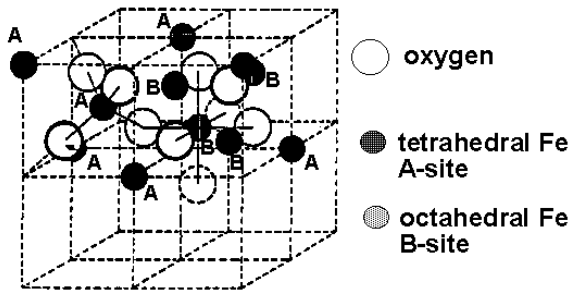

Fig. 1. A general structural diagram of a spinel structure.

Results and discussion

Phase formation

Fig. 2(a) shows the X – ray diffraction patterns of as synthesized $Ni_{0.5}Zn_{0.5}Gd_xFe_{2-x}O_4$ (where x = 0.1, 0.2, 0.3) at room temperature. The broad diffraction peaks indicate the poor crystallinity with nano-scaled ultrafine nature. However, all the peaks perfectly match with the crystalline phase of cubic spinel structure of Ni-Zn ferrite (JCPD Card No. 008-0234). It is also clear from **Fig. 2(a)** that with increase in Gd^{3+} concentration, the peak broadening decreases which indicates the increase in crystallite size. To understand this more precisely, a slow scan (0.002^0/sec) of selected diffraction peaks (220), (311), (400), (422), (511) and (440) was recorded to calculate the crystallite size. The crystallite size and strain induced in this polycrystalline

Table 1. Effect of Gd^{3+} ion concentration on structural parameters.

Composition	X (nm)	(a) (Å)	D_x (gm/cm^3)	Strain
Gd(0.1)	7.8	8.4208	5.514	-0.03005
Gd(0.2)	8.6	8.4348	5.710	-0.06999
Gd(0.3)	9.7	8.4553	5.892	-0.16723

Table 2. Various parameters calculated from EPR spectra of as synthesized $Ni_{0.5}Zn_{0.5}Gd_xFe_{2-x}O_4$ (where x = 0.1, 0.2, 0.3) nano particles.

Composition	g - value	ΔH_{pp}	Spin Concentration (N_S)	Relaxation Time (τ_S)
Gd(0.1)	2.04507	1050.3	2.17×10^{15}	6.116×10^{-15}
Gd(0.2)	2.00923	532.6	5.49×10^{14}	1.228×10^{-14}
Gd(0.3)	2.01635	511.4	4.81×10^{14}	1.274×10^{-14}

Table 3(a). Table showing the g – value, Line width Spin concentration and relaxation time for $Ni_{0.5}Zn_{0.5}Gd_{0.1}Fe_{1.9}O_4$ nanoparticles.

Composition	g - value	ΔH_{pp}	Spin Concentration (N_S)	Relaxation Time (τ_S)
Raw	2.04507	1050.3	2.17×10^{15}	6.116×10^{-15}
573 K	2.16997	981.2	1.70×10^{15}	6.170×10^{-15}
773 K	2.22448	1098.7	2.28×10^{15}	5.375×10^{-15}
973 K	2.40785	1306.0	1.78×10^{15}	4.178×10^{-15}

Table 3(b). Table showing the g – value, Line width Spin concentration and relaxation time for $Ni_{0.5}Zn_{0.5}Gd_{0.2}Fe_{1.8}O_4$ nanoparticles

Composition	g - value	ΔH_{pp}	Spin Concentration (N_S)	Relaxation Time (τ_S)
Raw	2.00923	532.6	5.49×10^{14}	1.228×10^{-14}
573 K	2.02074	677.2	5.89×10^{14}	9.60×10^{-15}
773 K	2.09472	739.4	7.12×10^{14}	8.482×10^{-15}
973 K	2.24607	1002	1.02×10^{15}	5.837×10^{-15}

Table 3(c). Table showing the g – value, Line width Spin concentration and relaxation time for $Ni_{0.5}Zn_{0.5}Gd_{0.3}Fe_{1.7}O_4$ nanoparticles

Composition	g - value	ΔH_{pp}	Spin Concentration (N_S)	Relaxation Time (τ_S)
Raw	2.01635	511.4	4.81×10^{14}	1.274×10^{-14}
573 K	2.04516	656.5	6.65×10^{14}	9.784×10^{-15}
773 K	2.06526	753.2	8.33×10^{14}	8.445×10^{-15}
973 K	2.19718	1257.7	1.80×10^{15}	4.754×10^{-15}

material was calculated from Williamson-Hall method; $\beta \cos\theta = 4 \in \sin\theta + \lambda/D$ where D is the crystallite size, λ is the wavelength of the X-ray, β is full width at half maximum (FWHM) measured in radians, $\in$ is the induced strain in system, and θ is the Bragg angle. The average crystallite size varied between 7.8 to 9.7 nm with the increase of Gd^{3+} concentration from 0.1 to 0.3.

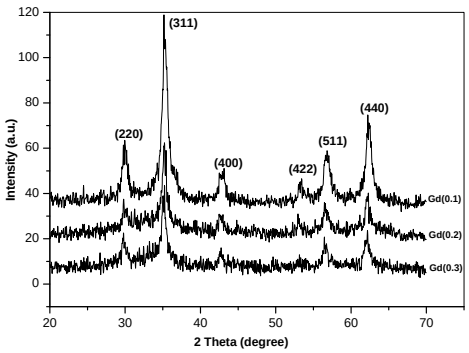

Fig. 2(a). XRD patterns of $Ni_{0.5}Zn_{0.5}Gd_xFe_{2-x}O_4$ (where x = 0.1, 0.2, 0.3) nano particles at room temperature.

Furthermore, to study the effect of heating on dimensions of nanoparticles, the samples were annealed at 573 K, 773 K and 973 K for 2 hrs to see changes in their physical properties.

Fig 2(b) shows XRD patterns of $Ni_{0.5}Zn_{0.5}Gd_{0.1}Fe_{1.9}O_4$ annealed nanoparticles.

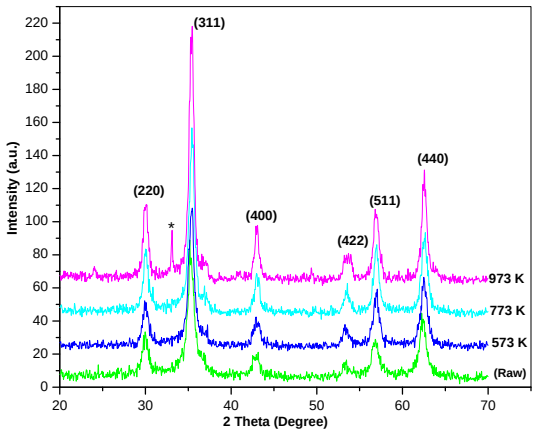

Fig. 2(b). XRD patterns of $Ni_{0.5}Zn_{0.5}Gd_{0.1}Fe_{1.9}O_4$ annealed at different temperatures. * denotes the secondary phase at 973 K.

The peak sharpness increase with annealing temperature indicates the growth in crystallite size. Similar behaviour is observed in other two compositions too. This is attributed to the grain growth of particles in the nano region at temperatures well below the melting temperature of the bulk ferrites [**14**]. Hence at very low temperature, the large number of atoms on the surface of the particles joins with their neighboring boundaries and leads to grain growth, which in turn alters the physical properties of the material. In finite size particles and a strain occurs due to negative pressure imposed due to replacement of Fe^{3+} ions by Gd^{3+} ions [**14**]. The X – ray density (D_x) and induced lattice strain due to replacement of Fe^{3+} ions by Gd^{3+} ions is calculated and shown in **Table 1**. It is clear (**Table 1**) that the value of crystallite size, lattice parameter and X-ray intensity increases with the increase of Gd^{3+} concentration (also shown in **Fig. 3**). This increase is because of the larger ionic radii of the Gd^{3+} (0.938 Å) ions as compared to Fe^{3+} (0.6459 Å) ions occupying octahedral sites [**15**].

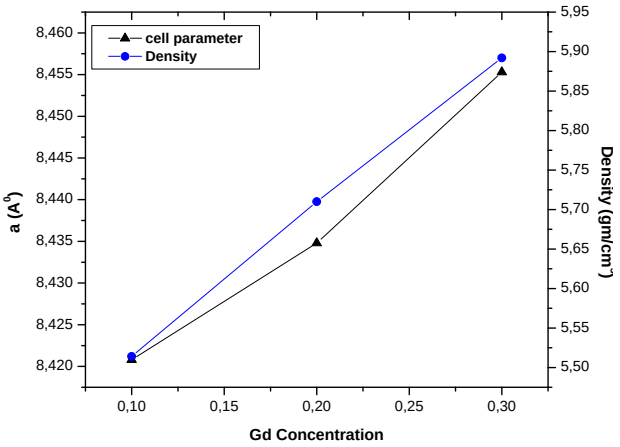

Fig. 3. Variation of lattice parameter and X – ray density with Gd^{3+} concentration in Ni – Zn ferrite.

Structure and microstructure

A detailed high resolution transmission electron microscopy experiments were performed to reveal the nano – scaled features of Gd^{3+} doped Ni – Zn ferrite system in real and reciprocal space. It was noted that the addition of Gd^{3+} (0.1, 0.2 and 0.3 wt.%) the basic microstructure of Ni – Zn ferrite leads to increase in the size of the nanoparticles (**Fig. 4**). These nanoparticles are random in shape with normally a facetted morphology with sharp edges and vertices (**Fig. 4(a), (b) and (c)**). The average size of particles was noted about 15, 21 and 25 nm for $Ni_{0.5}Zn_{0.5}Gd_{0.1}Fe_{1.9}O_4$, $Ni_{0.5}Zn_{0.5}Gd_{0.2}Fe_{1.8}O_4$ and $Ni_{0.5}Zn_{0.5}Gd_{0.3}Fe_{1.7}O_4$ respectively (**Fig. 4**).

The differences in size range of crystallites and particles of the material points towards the presence of amorphous layer at the surface of nanoparticles. For higher Gd^{3+} content, the difference becomes even larger. It may be due to the increase in defect at core of nanoparticle. **Fig. 5** further elucidates that the size distribution of nanoparticles in all three conditions is significantly narrow with an asymptotic nature.

However in most of the instances, since the particles were in aggregate with a cluster – formation, the measurement of individual particle size was a cumbersome to distinguish the contours of the periphery of the particles among themselves. Crystallographic interpretations of these samples were carried out in reciprocal space by recording the corresponding selected area electron diffraction patterns (SAEDPs).

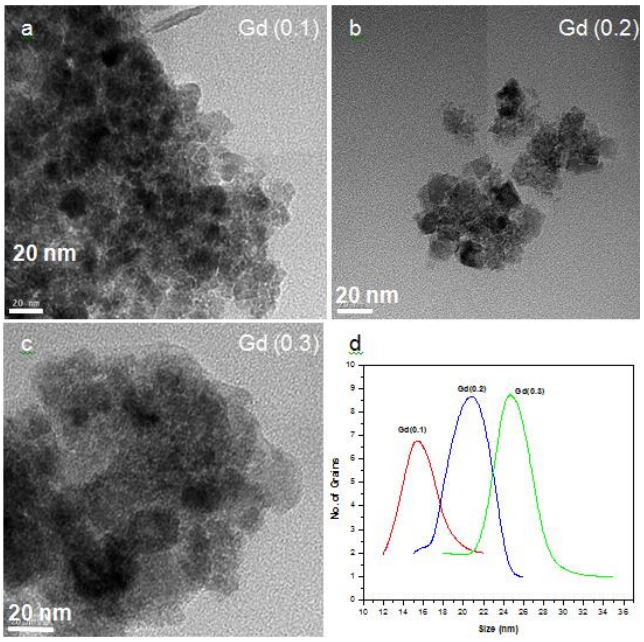

Fig. 4. HRTEM images of nanoparticles: (a) $Ni_{0.5}Zn_{0.5}Gd_{0.1}Fe_{1.9}O_4$ (b) $Ni_{0.5}Zn_{0.5}Gd_{0.2}Fe_{1.8}O_4$ (c) $Ni_{0.5}Zn_{0.5}Gd_{0.3}Fe_{1.7}O_4$ and (d) corresponding size distribution curve for $Ni_{0.5}Zn_{0.5}Gd_xFe_{2-x}O_4$ (where x = 0.1, 0.2, 0.3) nanoparticles.

Fig. 5(a) shows a SAEDP of $Ni_{0.5}Zn_{0.5}Gd_{0.1}Fe_{1.9}O_4$ from an aggregate of nanoparticles. A set of five important Debye rings corresponding to hkl planes: 220 (d = 0.29 nm), 311 (d = 0.25 nm), 400 (d = 0.21 nm), 511 (d = 0.16 nm) and 440 (d = 0.15 nm) of the basic Ni – Zn ferrite cubic crystal structure (space group: Fd $\bar{3}$m, a = 8.399 Å) are marked in **Fig. 5(a).** These Debye rings are continuous and diffused, which further corroborate that the material is in nano – scale with a structure consisted of presumably a significant fraction of defects at sub – nano scale. Similar SAEDPs were recorded in case of other two samples i.e., $Ni_{0.5}Zn_{0.5}Gd_{0.2}Fe_{1.8}O_4$ and $Ni_{0.5}Zn_{0.5}Gd_{0.3}Fe_{1.7}O_4$ (**Fig. 5(b) and 5(c)**). However, in this case (Fig. 5(b) & (c)), the Debye rings are decorated with fine spots which are attributed to the increase in average size of nanoparticles from 15 nm ($Ni_{0.5}Zn_{0.5}Gd_{0.1}Fe_{1.9}O_4$) to 21 nm ($Ni_{0.5}Zn_{0.5}Gd_{0.2}Fe_{1.8}O_4$) and finally to 25 nm ($Ni_{0.5}Zn_{0.5}Gd_{0.3}Fe_{1.7}O_4$), leading to improvement in crystallinity. Since the basic crystalline Ni-Zn ferrite cubic structure remains the same in all three Gd^{3+} doped conditions, the planes (hkl) of first sample: $Ni_{0.5}Zn_{0.5}Gd_{0.1}Fe_{1.9}O_4$ (**Fig. 4a**), are only marked on the SAEDP. We do not see any new planes in the SAEDP emerging due to increase of Gd^{3+} content in Ni-Zn ferrite.

Electron paramagnetic resonance measurements

X-band EPR spectra recorded at ambient temperature for different Gd^{3+} concentration doped Ni-Zn ferrite raw and

annealed nanoparticles are shown in **Fig. 6(a), (b), (c) and (d)**. The 1, 1 Diphenyl 2-picryl hydrazyl (DPPH) has been used as standard reference material for g-value and spin concentration calculations.

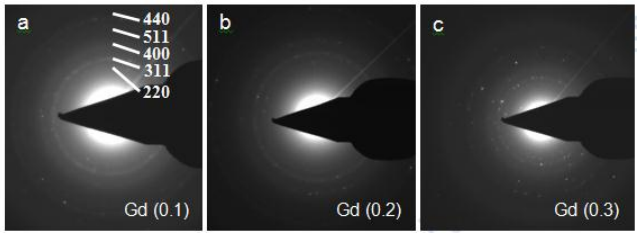

Fig. 5. SAEDPs recorded from nanoparticles: (a) $Ni_{0.5}Zn_{0.5}Gd_{0.1}Fe_{1.9}O_4$ (b) $Ni_{0.5}Zn_{0.5}Gd_{0.2}Fe_{1.8}O_4$ and (c) $Ni_{0.5}Zn_{0.5}Gd_{0.3}Fe_{1.7}O_4$.

At room temperature, a single, strong and symmetric broad EPR signal was observed for both raw and annealed $Ni_{0.5}Zn_{0.5}Gd_xFe_{2-x}O_4$ (where x = 0.1, 0.2, 0.3) ferrite nanoparticles with varying g-values in the range 2.0092 to 2.0200 and 2.0207 to 2.4079, respectively.

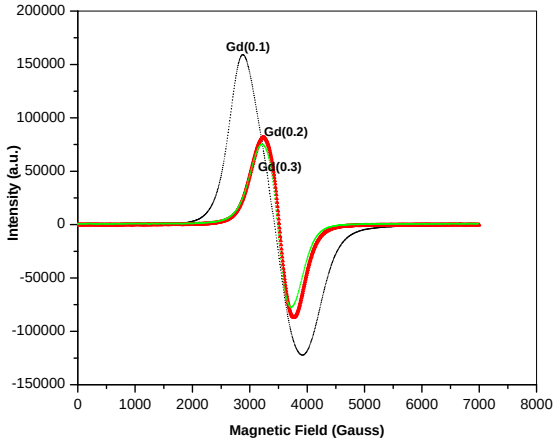

Fig. 6 (a). EPR spectra of as synthesized $Ni_{0.5}Zn_{0.5}Gd_xFe_{2-x}O_4$ (where x = 0.1, 0.2, 0.3) nano particles at ambient temperature.

The g value of the EPR signal is a function of the molecular motion, the paramagnetic properties and the symmetry of ions in a material [**16-19**]. All the spectra were analyzed using Lorentzian distribution function to obtain the values of various parameters such as peak-to-peak line width (ΔH_{pp}), g-value, spin concentration (N_S) and relaxation time (T_2). As the concentration of Gd^{3+} is increased, the line narrows down and shifts to higher resonance fields. The peak-to-peak line width (ΔH_{pp}) behaviors for unannealed samples decreases with increase in Gd^{3+} ions concentration as shown in **Fig. 6** (also shown in **Table 2**).

This exhibits due to decrease in the dipolar interaction and increase in super exchange interactions which lead to narrowing of the resonance signal explaining the reduction in ΔH_{pp} as shown in **Fig. 6(a).** The g-value of raw samples is decreased from 2.04507 to 2. 00923 confirming the increase in particle size, with Gd^{3+} ions concentration [**15**]. The increase in relaxation time with increase in Gd^{3+}, may be due to the enhanced exchange bias interaction between ferromagnetic core and antiferromagnetic surface layer. This point also gets support from XRD and HRTEM data.

The resonance line width, g-values and spins concentration increases linearly in 573, 773 and 973 K annealed samples. The line width is maximum in 973 K in all the samples. The increase in the line width for annealed samples is originating from increased dipolar - dipolar interactions among multidomain particles formed at high temperatures, as domain magnetic moments are more randomly oriented in multidomain particles.

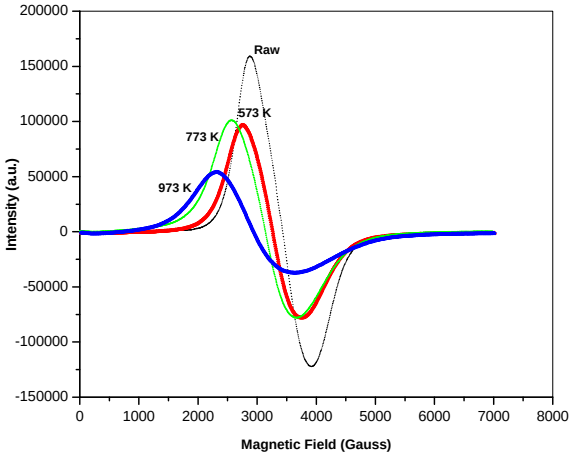

Fig. 6(b). EPR spectra of $Ni_{0.5}Zn_{0.5}Gd_{0.1}Fe_{1.9}O_4$ annealed at different temperatures.

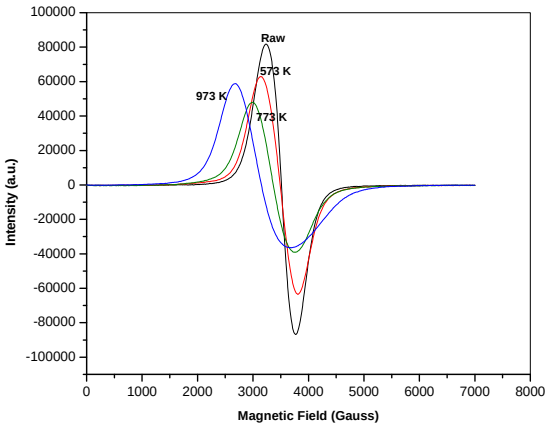

Fig. 6(c). EPR spectrum of of $Ni_{0.5}Zn_{0.5}Gd_{0.2}Fe_{1.8}O_4$ nanoparticles annealed at different temperatures.

However spin disorder (frustration) arises from antiferromagnetic interactions between the neighboring spins in magnetic Gd^{3+} doped Ni-Zn ferrite of annealed samples.

The antiferromagnetic interactions between the magnetic clusters also enhance this frustration. Since the intrinsic effective magnetic moment (local magnetization) decreases in annealed sample, the dipolar field increases in parallel which causes inhomogeneity in the sample annealed at higher temperatures. This can be related to the behavior of the whole system as a solid with respect to magnetism and the disordered and frozen spin profile to EPR. For annealed nanoparticles the surface anisotropy was observed which causes additional disorder depending on the morphology of the particle. This causes increase in line

with values shift as a whole to higher resonance magnetic field value [**20**].

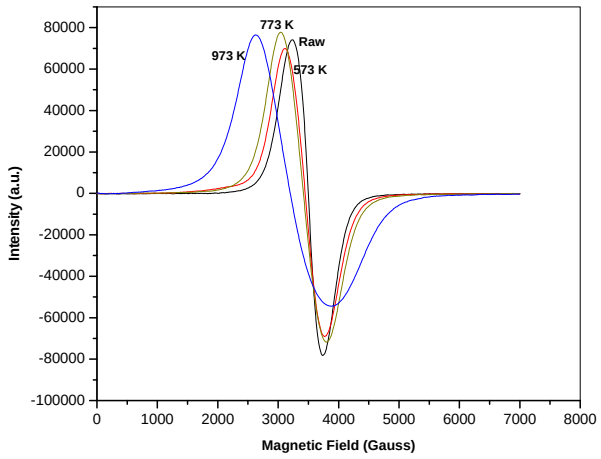

Fig. 6(d). EPR spectrum of of $Ni_{0.5}Zn_{0.5}Gd_{0.3}Fe_{1.7}O_4$ nanoparticles annealed at different temperatures.

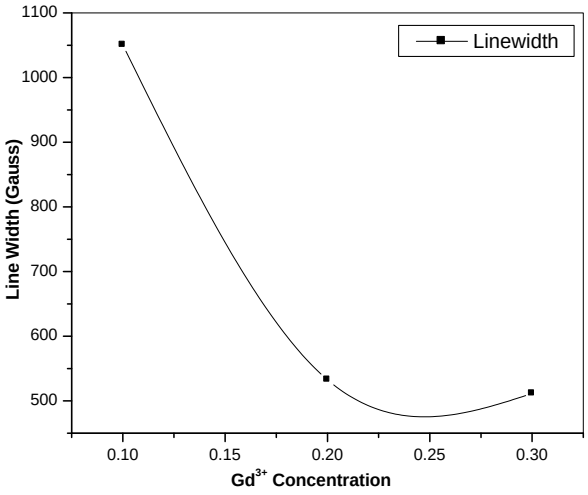

Fig. 7. Variation of line width with Gd^{3+} concentration in Ni – Zn ferrite.

The effect of annealing temperature on resonance field values (**Fig. 8**) shows the strong temperature dependence. As the annealing temperature increases the resonance field (H_y) decreases. The amount of shift in resonance curve is in the range of ~300 G to 700 G in 0.1 Gd^{3+} and 0.3 Gd^{3+} Ni-Zn ferrite at 973 K annealed samples respectively (See **Table 3 (a), (b)** and **(c)**). The resonance field values for the annealed samples remains always greater than that of unannealed (raw) samples as observed in the line width curves (**Fig. 8**). This shift is attributed to increase in microscopic fields accompanied by a decrease in the external resonance field in annealed samples reveals line broadening and a decrease in the signal intensity in higher Gd^{3+} concentration doped samples [**20**]. The spin concentration is calculated by the comparison method using DPPH standard reference material are listed in **Table 3** (a), (b) and (c) for raw and annealed $Ni_{0.5}Zn_{0.5}Gd_xFe_{2-x}O_4$ (where x = 0.1, 0.2, 0.3) nanoparticles. Superexchange interaction should decrease due to the defect introduced by presence of Gd^{3+}. As a result spin concentration in non-annealed samples decrease with increasing Gd^{3+} concentration. While on annealing, spin concentration may increase due to movement of frustrated Gd^{3+} ions from core to the surface of nanoparticles.

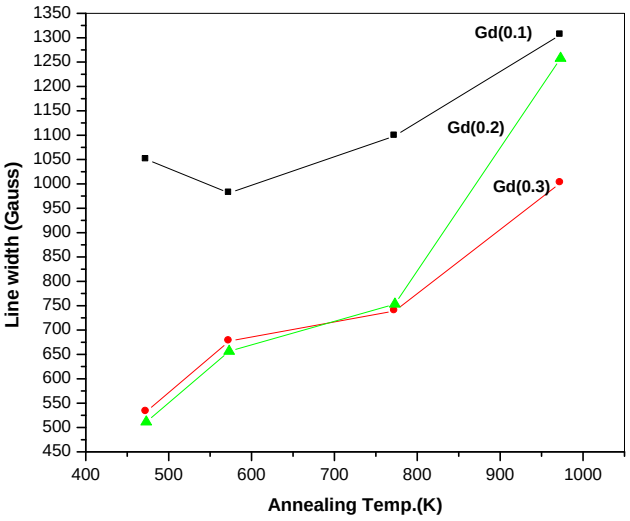

Fig. 8. Effect of annealing at different temperatures on line width in $Ni_{0.5}Zn_{0.5}Gd_xFe_{2-x}O_4$ (where x = 0.1, 0.2, 0.3) nano particles.

Conclusion

Ultrafine nanoparticles of $Ni_{0.5}Zn_{0.5}Gd_xFe_{2-x}O_4$ (where x = 0.1, 0.2, 0.3) ferrite were successfully developed by co precipitation method. XRD studies of these nanoparticles reveal the distortion in the spinel lattice structure induced due to large ionic radii of Gd^{3+} ions at the octahedral Fe^{3+} ions site. The calculated values of crystallite size and particle size from XRD and HRTEM exhibits the correlation between the data of both measurements. EPR spectra confirm the ferromagnetic behaviour of these nanoparticles due to higher order of dipolar-dipolar interaction. On increasing Gd^{3+} ions concentrations in sample the narrowing of signal is observed which explains the increase in super exchange interaction i.e. movement of electron among Gd^{3+}-O- Fe^{3+} in the core group and the spin biasing in the glass layer.. The decrease in g value and increase in relaxation time is correlated with increase in particle size as Gd^{3+} ions concentration increases in Ni-Zn ferrite nanoparticles.

Acknowledgements

Director, National Physical Laboratory, New Delhi is acknowledged for permission to carry out this work. Balwinder Kaur is thankful to J&K State Council for Science & Technology, Department of Science and Technology, J & K and Higher Education Department, J & K for Young Scientist Fellowship – 2009.

Reference

1. Popovici, M.; Savii, C.; Niznansky, D.; Subrt, J.; Bohacek, J.; Becherescu, D.; Caizer, C.; Enache, C.; Ionescu, C. *J. Optoelectron. Adv. Mater.* **2003**, *5*, 251.
2. Shinkai, M. *J. Biosci. Bioeng.* **2002**, *94*, 606. **DOI**: 10.1016/S1389-1723(02)80202-X
3. Lubbe, A.S.; Alexiou, C.; Bergemann, C. *J. Surgical Res.* **2001**, *95*, 200. **DOI**: 10.1006/jsre.2000.6030
4. Tiefenauer, L.X.; Tschirky, A.; Kuhne, G.; Andres, R.Y. *Magn. Res. Imaging*, **1996**, *14* 391. **DOI**: 10.1016/0730-725X(95)02106-4

5. Skmoski, R. *J. Phys.: Condens. Matter*. **2003**, *15*, R841. **DOI**: 10.1088/0953-8984/15/20/202
6. Gibbs, M.R.J. *Curr. Opin. Solid State Mater. Sci.* **2003**, *7*, 83. **DOI**: 10.1016/S1359-0286(03)00053-6
7. Banerjee, S. K., and B. M. Moskowitz, Ferrimagnetic properties of magnetite, in *Magnetite Biomineralization and Magnetoreception in Organisms: A New Magnetism*, vol. edited by J. L. Kirschvink, and e. al., pp. 17-41, Plenum Publishing Corporation, **1985**.
8. Chen, J.P.; Sorenson, C.M.; Klabunde, K.J.; Hadjipanayis, G.C., Devlin, E.; Kostikas, A. *Phys. Rev. B*, **1996**, *54*, 9288. **DOI**: 10.1103/PhysRevB.54.9288
9. Adriana, S.A.; Jose, D.A.; Waldemar, A.A.M.; Maria, C.M.A.; *J. Appl. Phys.*, **2000**, *87*, 4352. **DOI**: 10.1063/1.373077
10. *Rezlescu, N.; Rezlescu, E.; Pasnicu, C.; Craus, M.L. J.* Phys.: Condens. Matter., ***1994***, 6, *5707*. **DOI**: 10.1088/0953-8984/6/29/013
11. Rezlescu, N.; Rezlescu, E.; Pasnicu, C.; Craus, M.L. *J. Magn. Magn. Mat.* **1994**, *136*, 319. **DOI**: 10.1016/0304-8853(94)00309-2
12. Rezlescu, N.; Rezlescu, E. *Solid State Commun.* **1993**, *88*, 139. **DOI**: 10.1016/0038-1098(93)90395-4
13. Shahane, G.S.; Kumar, Ashok; Arora, Manju; Pant, R.P.; Lal, Krishan. *J. Magn. Magn. Mater.* **2010**, *322*, 1015. **DOI**: 10.1016/j.jmmm.2009.12.006
14. B.D. Cullity, *Elements of X – ray Diffraction*, Adison – Wesley, London, **1059**, 261.
15. Kumar, V.; Rana, A.; Yadav, M.S.; Pant, R.P. *J. Magn. Magn. Mater*. **2008**, *320*, 1729. **DOI**: 10.1016/j.jmmm.2008.01.021
16. Pant, R.P.; Arora, Manju; Kaur**,** Balwinder; Kumar, Vinod; Kumar, Ashok. *J. Magn. Magn. Mater*. **2010**, *322*, 3688. **DOI**: 10.1016/j.jmmm.2010.07.026
17. Stucki, J.W.; Banwart, W.L. Reidel, Dordrecht, **1980**.
18. Wu, K.H.; Chang, Y.C.; Chen, H.B.; Yang, C.C.; Horng, D.N. *J. Magn. Magn. Mater*. **2004**, *278*, 156. **DOI**: 10.1016/j.jmmm.2003.12.331
19. Wu, K.H.; Huang, W.C.; Wang, G.P.; Wu, T.R. *Mater. Res. Bull.* **2005**, *40*, 1822. **DOI**: 10.1016/j.materresbull.2005.04.041
20. Wu, K.H.; Ting, T.H.; Li, M.C.; Ho, W.D. *J. Magn. Magn. Mater.* **2006**, *298*, 25. **DOI**: 10.1016/j.jmmm.2005.03.008
21. Koseoglu, Y.; Aktas, B. *Phys. Stat. Sol. (c)* **2004**, *1*, 3516. **DOI**: 10.1002/pssc.200405494

